Synthetic Metals 162 (2012) 1756–1761

Contents lists available at SciVerse ScienceDirect

Synthetic Metals

journal homepage: www.elsevier.com/locate/synmet

Investigations of optical properties of MEH-PPV/ZnO nanocomposites by photoluminescence spectroscopy

Ishaq Musa, Florian Massuyeau, Eric Faulques [1], Thien-Phap Nguyen *,[1]

Institut des Matériaux Jean Rouxel, UMR6502 CNRS, Université de Nantes, 2 rue de la Houssinière, F-44322 Nantes, France

ARTICLE INFO

Article history:
Received 1 December 2010
Received in revised form
19 December 2011
Accepted 3 January 2012
Available online 8 February 2012

Keywords:
ZnO nanoparticles
MEH-PPV
UV–Vis spectroscopy
Photoluminescence spectroscopy
Time-resolved photoluminescence

ABSTRACT

The optical properties of hybrid composite films based on poly [2-methoxy-5-(2-ethyl-hexyloxy)-1,4-phenylene-vinylene] (MEH-PPV) and zinc oxide (ZnO) nanoparticles of various sizes (5–20 nm) and with different concentrations have been investigated. The steady-state and time-resolved photoluminescence (PL) spectroscopy have been performed on nanocomposite films at room temperature. The PL results showed a significant enhancement in intensity in nanocomposites when using low nanoparticle concentrations (<5% ZnO). The particle size also impacts on the emission intensity by a larger emission efficiency in thin films containing small particles. In addition, a decrease in the photoluminescence lifetime of MEH-PPV composites has been also observed. Analysis of the time resolved PL decay of nanocomposite films suggests an energy transfer process from the nanoparticles to the polymer chains, in agreement with the steady state measurements.

1. Introduction

Conjugated polymers containing inorganic nanoparticles have been the subject of considerable research because of their potential for optical, electrical, and photovoltaic applications [1–4]. Recent investigations of promising materials for organic light emitting diodes (OLEDs) have demonstrated that introducing n-type inorganic nanoparticles into conjugated polymers is efficient to produce stable and high performance devices [5]. Although the used nanoparticles are usually metal oxides (such as titanium or silicon oxides), their distribution inside the polymer matrix is such that the charge transport could be improved and the performance of the devices is improved. In particular, composites of n-type zinc oxide (ZnO) nanoparticles and p-type conjugated polymers are very interesting for UV LEDs and OLED applications. ZnO has strong absorption in the UV light range and therefore can be used to protect the devices from oxidation to increase the lifetime of organic devices [6,7]. Among the conjugated polymers which are used as active materials in OLEDs, poly [2-methoxy-5-(2-ethyl-hexyloxy)-1,4-phenylene-vinylene] (MEH-PPV) is used in numerous emitting devices thanks to its high stability and good electrical conductivity. Composites made of MEH-PPV and nanoparticles have been investigated to provide stable active materials in OLEDs in order to enhance their lifetime [8]. Using low particle concentrations, light emission by the composite film remains identical to that of the pristine polymer. It has been recently demonstrated that such composites have lower defect concentrations than those of polymer [9], which results in a better charge carrier transport and a better efficiency of devices. As ZnO (n-type) has higher electron mobility than hole mobility and conjugated polymer shows higher hole mobility than electron mobility, which makes electronic properties of both materials advantageous when mixing them together in order to improve the light emission efficiency [10].

In this paper we have investigated the optical properties of hybrid materials made of MEH-PPV loaded with ZnO nanocrystals of various sizes and concentrations. We delineate the optimal loading percentages of ZnO nanoparticles in the composite film by using both steady state and time-resolved photoluminescence (PL) techniques.

2. Experimental

2.1. Preparation of ZnO nanoparticles

Various sizes of ZnO nanoparticles (5–20 nm) were synthesized using different chemical routes.

Method I – ZnO nanoparticles with average size of about 20 nm were prepared from zinc nitrate hydrate $Zn(NO_3)_2{\cdot}6H_2O$ (99%) and sodium hydroxide (NaOH) according to the procedure previously reported by Uekawa et al. [11]. An amount of 22.536 mg of zinc nitrate hydrate and 3.09 mg of NaOH were added to 100 mL of

* Corresponding author. Tel.: +33 2 40 37 39 76; fax: +33 2 40 37 39 91.
E-mail address: Thien-Phap.Nguyen@cnrs-imn.fr (T.-P. Nguyen).
[1] These authors contributed equally to this work.

0379-6779/$ – see front matter © 2012 Elsevier B.V. All rights reserved.
doi:10.1016/j.synthmet.2012.01.011

distilled water (DW) separately. Zinc nitrate hydrate and sodium hydroxide were stirred until the powder dissolves completely in DW. The mixture was centrifuged for 20 min. The supernatant liquid was removed in order to keep the precipitated powder. A small amount of DW is added to it (equivalent to 5% of the total volume amount) in a vessel which was shaken until a white and viscous product is formed. The mixture ($Zn(OH)_2 + H_2O$) was stirred and heated at a temperature of 75 °C for 2 h, then centrifuged to separate the supernatant from the precursor (ZnO_2). The precipitated products (ZnO_2) were washed twice with ethanol, then dried, and heated at 220 °C for 2 h to obtain the ZnO nanoparticles.

Method II – Colloidal solutions of ZnO nanoparticles (5 nm in diameter) were obtained according to the method described elsewhere [12,13]. Briefly, an amount of 5.5 g of zinc acetate dehydrate (98+%, Sigma Aldrich) in 250 mL of ethanol was heated until the solution became clear. This solution was refluxed for 1 h, and 150 mL of the solvent was removed by distillation and replaced by the same amount of fresh ethanol. After, 1.39 g of lithium hydroxide monohydrate (Aldrich) was added to the solution in an ultrasonic bath at 0 °C. The mixture was dispersed for 2 h to obtain a transparent solution consisting of ZnO nanoparticles in suspension with apparent diameters of about 5 nm, respectively. The solution was filtered through a 0.1 μm membrane filter to remove undissolved LiOH.

To synthesize ZnO nanoparticles of 10 nm diameter, the method of Hoyer was used [14,15]. The solution containing the 5 nm particles was heated and mixed with 5% of deionized water at 60 °C for 10 min. During this procedure, a white powder was formed and precipitated, and then the solution was centrifuged to recover the precipitate. Afterward, the product was washed with an ethanol–water mixture (19:1) and again centrifuged. The last step was repeated four times to remove physisorbed ionic compounds.

2.2. Elaboration of nanocomposite materials

The MEH-PPV was purchased from (Aldrich) and used without purification. In the preparation of hybrid materials, the ZnO nanoparticles with various sizes (5, 10 and 20 nm) were dispersed in toluene, and the MEH-PPV solution was prepared by dissolving MEH-PPV in toluene with a concentration of 10 mg/mL. Solutions of hybrid materials with 0, 2, 5, 10, and 20 wt% ZnO were obtained by mixing the required amount of ZnO nanoparticles with MEH-PPV solution and subjected to ultrasonic treatment for 4 h to improve the dispersion of ZnO nanoparticles. Thin-films of hybrid material were prepared by spin coating the solution on glass substrates. The samples were dried and kept in vacuum. UV–visible absorption spectra of composite films were obtained using a Varian Cary Scan UV–Vis spectrophotometer. Steady state PL spectra were collected from the front face geometry of the samples with a Jobin-Yvon Fluorolog spectrometer using a xenon lamp (500 W) as an excitation source. Ultrafast PL experiments were carried out with a regenerative amplified femtosecond laser system (Spectra Physics Hurricane X) delivering 100 fs pulses at 1 kHz, 800 nm, and 1 W mean power. Composite samples were excited at 267 nm by triple harmonic generation. Transient signals were spectrally dispersed into an imaging spectrograph. The time-resolved emission spectra were detected with a streak camera of temporal resolution < 20 ps.

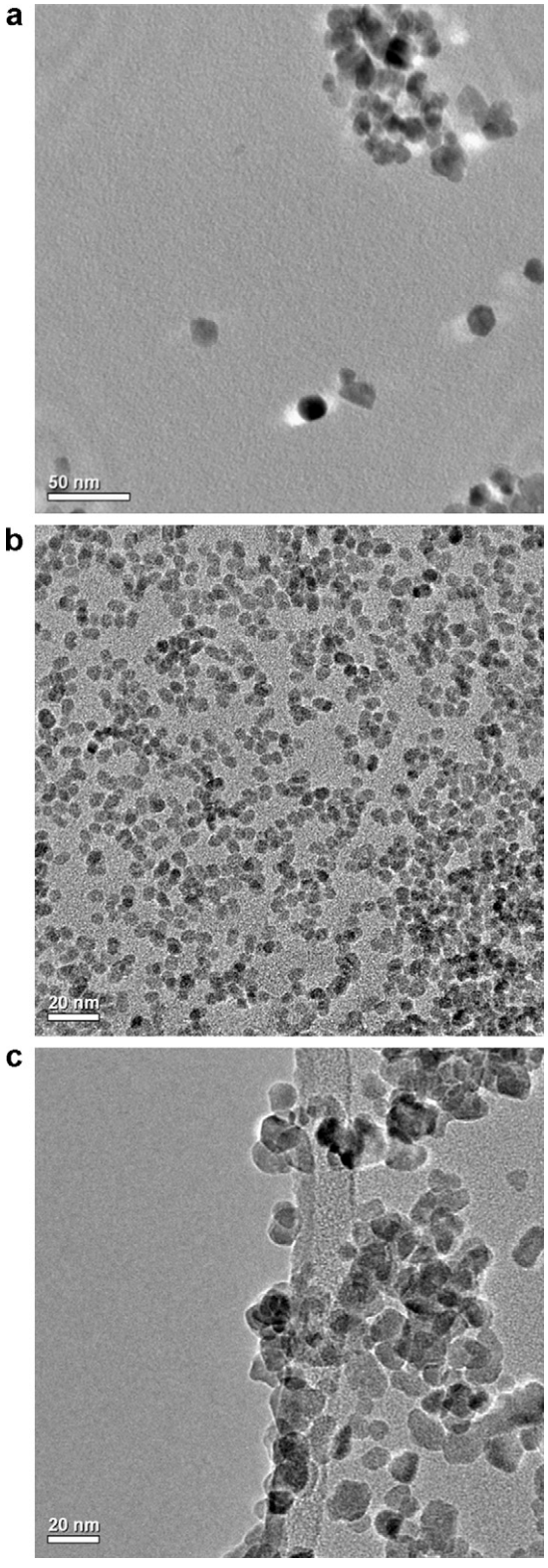

Fig. 1. (a) TEM image for MEH-PPV–ZnO nanocomposites corresponding to 20 nm nanoparticles and 10% concentration, and TEM images of ZnO nanoparticles of sizes: (b) 5 nm, (c) 10 nm.

3. Results and discussion

A transmission electron microscopy (TEM) picture for MEH-PPV–ZnO composites with average particle size of 20 nm and 10 wt% concentration is displayed in Fig. 1(a). In this image, the ZnO particles have a characteristic hexagonal shape. Also, it can be noticed that these particles in some area are dispersed and others aggregate among of polymer. Representative TEM images of ZnO nanoparticles with apparent sizes 5 and 10 nm prepared by method II are presented in Fig. 1(b) and (c).The transient PL spectrum of ZnO nanoparticles of size 10 nm at room temperature is shown in Fig. 2. It is composed of a UV emission band and a broad emission band.

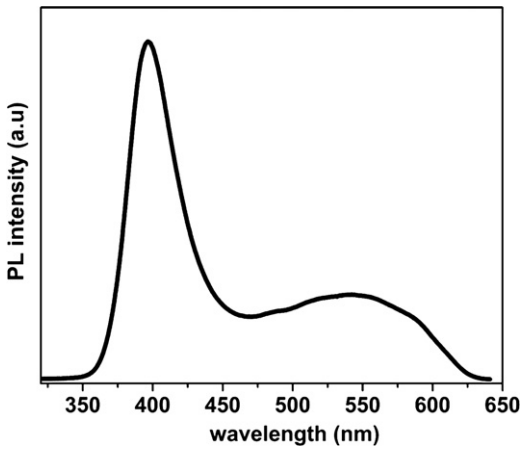

Fig. 2. Time-resolved PL spectrum (excitation: 267 nm) for ZnO nanoparticles of size 10 nm, integrated over a streak camera sweep of 1 ns.

The UV emission band is intense and centered at 396 nm, which is related to a near band-edge transition of ZnO. The broad emission band in the visible region of the spectrum between 450 and 610 nm, centered at 550 nm is linked to defects in ZnO. This band has been ascribed to several defects in the crystal structure of ZnO such as oxygen vacancies (V_o) or oxygen interstitial [16,17].

Fig. 3 shows the room-temperature UV–visible absorption of thin film composites with ZnO nanoparticles of various sizes (5, 10 and 20 nm) and concentrations (0, 2, 5, 10, and 20 wt%). The pristine MEH-PPV exhibits a broad absorption spectrum peaked at about 498 nm and ZnO nanoparticles have a sharp absorption edge at about 350, 355, and 365 nm for sizes 5, 10, and 20 nm respectively, as showed in insets of Fig. 3. It should be noted that the optical absorption increased in composites when the concentration of the ZnO nanoparticles increases up to a limit of <5% ZnO.

The transient PL spectra of the MEH-PPV/ZnO composite films with different concentrations (0, 2, 5, 10, and 20 wt%) and various sizes of ZnO nanoparticles (5, 10, and 20 nm) at room temperature are displayed in Fig. 4(a), (b), and (c), respectively. The spectrum of MEH-PPV shows the emission peaks centered at ~587 nm, and a shoulder at ~639 nm corresponding to the 0–0 and 0–1 vibronic transitions. Fig. 5 shows the steady state PL spectra of the MEH-PPV/ZnO composite films with different concentrations (0, 2, 5, 10, and 20 wt%) and ZnO nanoparticles of the size 5 nm at room temperature shown in Fig. 5. They present a behavior similar to transient PL measurements. It can be clearly observed from Figs. 4 and 5 that all thin film composites exhibit an enhancement of photoluminescence intensity, and a slight blue shift as the concentration of ZnO nanoparticles decreases. In the case of MEH-PPV/ZnO with size 5 nm, the intensity of PL increased even with high concentration of ZnO, while in MEH-PPV/ZnO with sizes 10 and 20 nm, the PL intensity of composite is quenched at high concentration (20 wt%). Fig. 6 illustrates the peak intensity dependence of composites films as a function of concentration of ZnO for different sized ZnO nanoparticles. From this figure, it can be observed that the PL emission is enhanced up to 2 wt% for all composites and then gradually decreases by increasing the concentration of ZnO nanoparticles. The PL enhancement of composites can be attributed to the strong interaction between the zinc oxide nanoparticles and conjugated polymer [18,19]. The quenching of PL emission of composites suggests that the ZnO nanoparticles provide an alternative pathway for relaxation of excited electrons and reduce the possibility of radiative emission of the excitons.

This alternative pathway is most likely to be a charge transfer based on the energy level alignment of MEH-PPV and ZnO nanoparticles. The LUMO of MEH-PPV is −3.0 eV and the HOMO

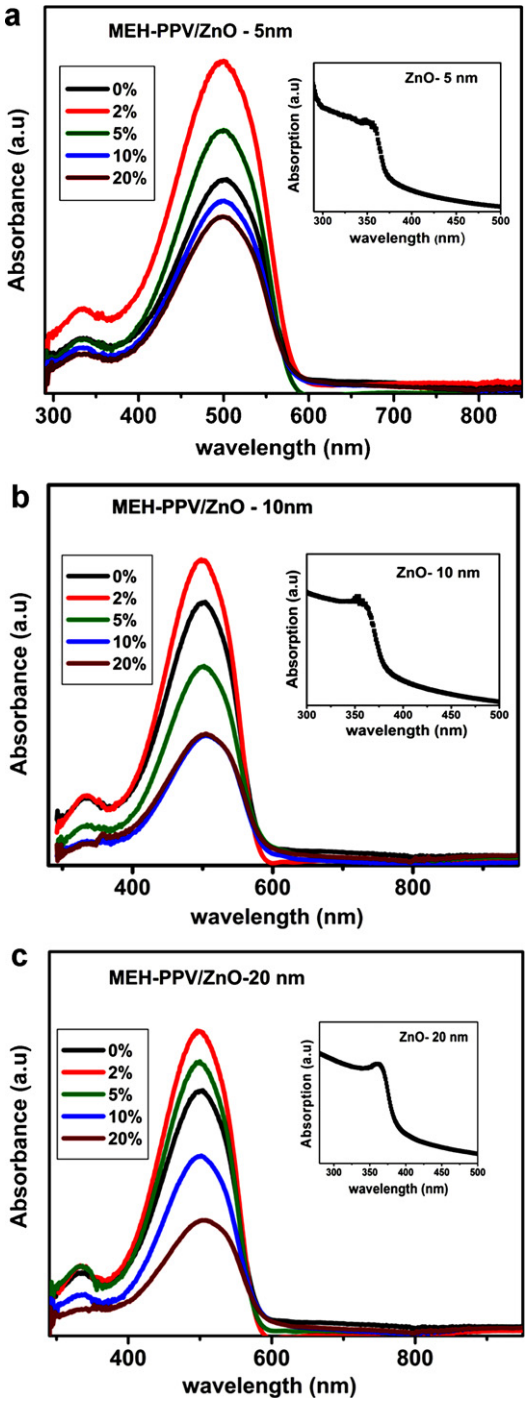

Fig. 3. Absorption spectra for thin films of pristine MEH-PPV and MEH-PPV/ZnO nanoparticle composites: (a) 5 nm, (b) 10 nm, and (c) 20 nm, of concentration from 2 to 20 wt% ZnO. Insets: absorption of ZnO nanoparticles.

is −5.3 eV. The conduction band of ZnO is −4.2 eV and the valence band is −7.6 eV. Therefore, the photoexcited excitons can dissociate at MEH-PPV and ZnO interfaces during the charge transfer process [20]. Additionally, it should be noted from the trends reported here that the small size of ZnO nanoparticles may play an important role in conjugated polymers in improving the performance of the PL emission.

It is also possible to trigger energy transfer from ZnO to the polymer by exciting the "green" defect band of ZnO around 550 nm as seen in Fig. 2. For time-resolved experiments, we excited the

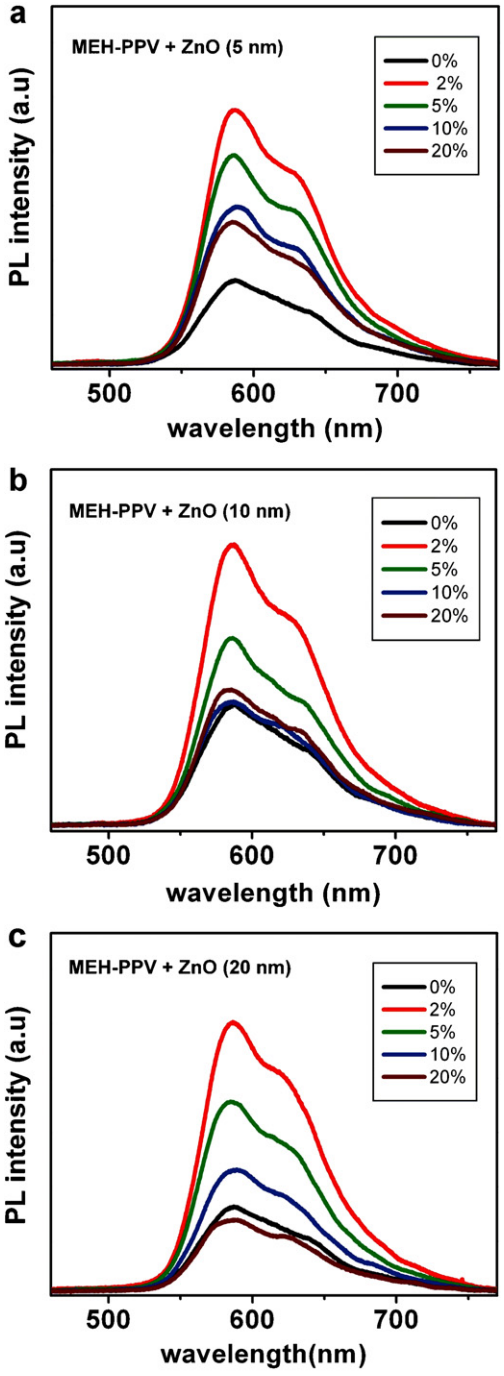

Fig. 4. Time-resolved PL spectra (excitation: 267 nm) for thin films of pristine MEH-PPV, and MEH-PPV/ZnO nanoparticle composites: (a) 5 nm, (b) 10 nm, and (c) 20 nm of concentration from 2 to 20 wt% ZnO. Time integration: 2 ns.

composite at 267 nm, and therefore we excite the ZnO nanoparticles by allowing energy transfer from the UV band.

In case of a resonant energy transfer between MEH-PPV and ZnO, one expects [21]:

(i) a decrease of the PL emission intensity of the donor, i.e. MEH-PPV;
(ii) a shortening of the PL lifetime of MEH-PPV.

In order to confirm the presence of energy transfer from MEH-PPV to ZnO nanocrystals, we measured the time-resolved PL decay of polymer composite films. Fig. 7 shows the PL kinetics of the

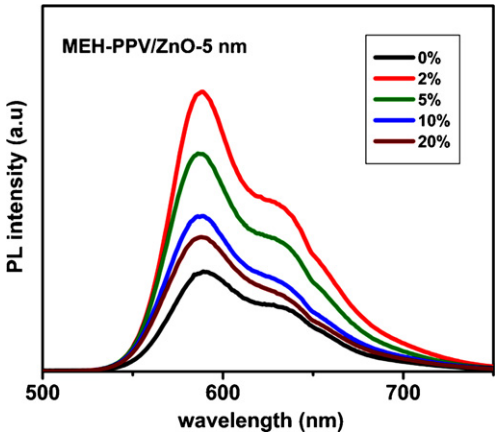

Fig. 5. Steady state PL spectra (excitation: 400 nm) for thin films of pristine MEH-PPV and MEH-PPV/ZnO nanoparticle composites with concentration varying from 2 to 20 wt% ZnO. Size of particles: 5 nm.

polymer matrix in a thin film of MEH-PPV/ZnO nanoparticles with size 20 nm and different concentrations (0 wt%, 2 wt%, 10 wt%, 20 wt%). The PL decays could be fitted by considering rate equations of exciton recombination from two excited states 1 and 2 with lifetimes τ_1, and τ_2 [22]. The fitting curves, indicated as solid lines in Fig. 7 are consistent with the experimental decay curves in the range 0–1 ns. The decaying population (n) can be expressed by:

$$n = A_1 n_1 + A_2 n_2$$

where n_1 and n_2 are the populations of excited states (levels 1 and 2, respectively), A_1, A_2 are proportional to the PL intensity from level 1 and level 2, respectively. The average decay time τ_{mean} can be defined according to Ref. [22]. The weight p_i corresponding to the relative population of photogenerated charges contributing to each of the decay times (A_i, τ_i) is calculated by $p_i = A_i\tau_i / \sum A_i\tau_i$ and is reported in parentheses next each decay component [22]. Results of lifetimes for MEH-PPV pristine and composites films are summarized in Table 1. From this table, the values of τ_2, and τ_{mean} of composite thin films decrease by increasing the concentration of ZnO nanoparticles in polymer. For the pristine MEH-PPV film, the lifetimes of the emission are $\tau_1 = 41$ ps, $\tau_2 = 173$ ps. For the composite film MEH-PPV/ZnO – 20 nm containing 2 wt% ZnO, the emission has lifetimes $\tau_1 = 80$ ps, $\tau_2 = 253$ ps. In the MEH-PPV/ZnO – 20 nm composite film loaded at 20 wt% ZnO, the lifetimes are $\tau_1 = 37$ ps, $\tau_2 = 153$ ps. It is clear that shorter lifetimes are observed in the case

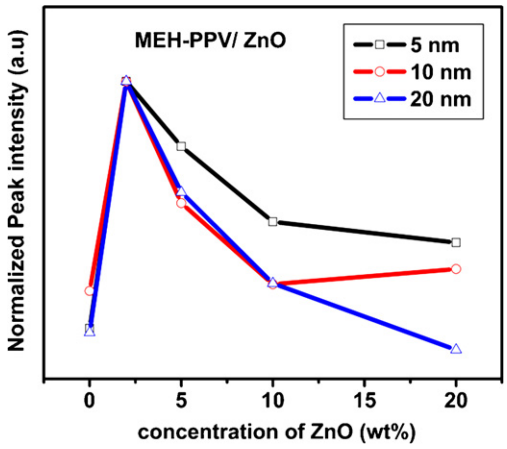

Fig. 6. Variation of PL peak intensity of composite thin films as a function of different concentrations of ZnO nanoparticles (0 wt%, 2 wt%, 5, 10 wt%, 20 wt%) and various sizes (5, 10, and 20 nm) (excitation: 267 nm).

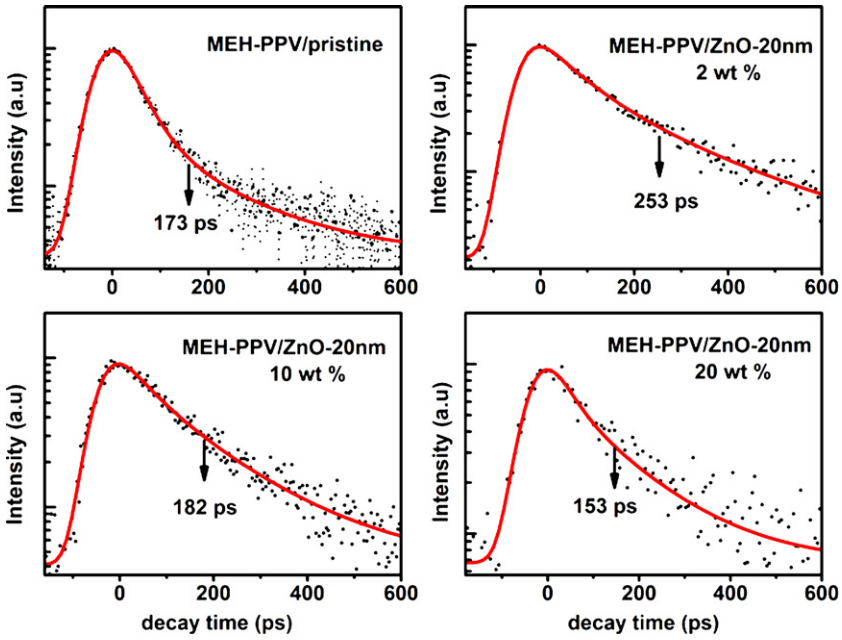

Fig. 7. Time-resolved PL kinetics (excitation: 267 nm) of (a) pristine MEH-PPV and composites containing (b) 2%, (c) 10%, and (d) 20%, ZnO 20-nm nanocrystals. The solid-lines are the fitting results of the kinetics using the model described in the text. The decay times for 0, 2, 10, and 20 wt% composites are τ_2 = 173 ps, 253 ps, 182 ps, and 153 ps, respectively. Decays are extracted from full streak camera images.

Table 1
PL decay times (τ_1, τ_2, τ_{mean}), percentage contributions $p_{1,2}$ to the emission of levels 1 and 2 (in parentheses), and relative exponential weight (A_1/A_2) for the transient PL of the different samples investigated. The sample list is ordered according to the notation of Fig. 7.

Samples	A_1/A_2	τ_1 (ps)	τ_2 (ps)	τ_{mean} (ps)
MEH-PPV – 0 wt%	9.9	41 (70%)	173 (30%)	80
MEH-PPV/ZnO – 2 wt%	4.03	80 (56%)	253 (44%)	156
MEH-PPV/ZnO – 5 wt%	3.076	53 (48%)	220 (52%)	140
MEH-PPV/ZnO – 10 wt%	2.991	66 (52%)	182 (48%)	121
MEH-PPV/ZnO – 20 wt%	3.14	37 (43%)	153 (57%)	103

of pristine MEH-PPV and highly concentrated composite (20 wt% of ZnO). On the other hand composites with different concentrations of ZnO (2, 5, 10 wt%) have longer decays. Fig. 8 compiles the PL decay time τ_{mean} of all polymer composite films as a function of concentration and size of ZnO. From this figure, we can conclude that as the ZnO concentration increases the PL decay of the composites becomes faster. This indicates that a Förster resonant energy transfer is likely to occur between the MEH-PPV and nanoparticles in composites thin films [21]. These results agree with other reports of PL lifetime decay in similar systems [23].

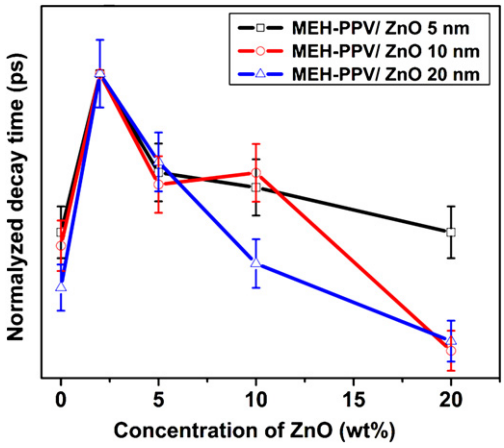

Fig. 8. Variation of PL decay times of composite thin films as a function of different concentrations of ZnO nanoparticles (0 wt%, 2 wt%, 5, 10 wt%, 20 wt%) and various sizes (5, 10, and 20 nm).

4. Conclusion

We have studied the effect of the various sizes and concentrations of hybrid MEH-PPV–ZnO composites on their optical properties. The PL spectra showed a significant enhancement in intensity in composites when using low nanoparticle concentrations (<5% ZnO). Additionally, it was also observed that the smaller the size of ZnO nanoparticles the higher the emission efficiency in thin films composites. Finally, the PL of MEH-PPV composites containing high concentrations of ZnO nanoparticles showed a drastic decrease in lifetime compared to composites with lower concentrations. The PL decay time of the 20% composite is even shorter than that of the pristine polymer. Shorter lifetimes in highly concentrated polymer composites indicate an electronic interaction between the polymer chains and the ZnO nanoparticles. In this case, shorter lifetimes can be ascribed to an energy transfer between nanoparticles and polymer chains promoting nonradiative recombination pathways.

References

[1] A.A. Lutich, G. Jiang, A.S. Susha, A.L. Rogach, F.D. Stefani, J. Feldmann, Nano Lett. 9 (2009) 2636–2640.
[2] A.J. Breeze, Z. Schlesinger, S.A. Carter, P.J. Brock, Phys. Rev. B 64 (2001) 125205.
[3] J.H. Warner, A.R. Watt, E. Thomsen, N. Heckenberg, P. Meredith, H. Rubinsztein-Dunlop, J. Phys. Chem. B 109 (2005) 9001–9005.
[4] Y.T. Lin, T.W. Zeng, W.Z. Lai, C.W. Chen, Y.Y. Lin, Y.S. Chang, W.F. Su, Nanotechnology 17 (2006) 5781–5785.
[5] M.V.M. Rao, Y.K. Su, T.S. Huang, M.L. Tu, S.S. Wu, C.Y. Huang, J. Electrochem. Soc. 157 (2010) H832–H836.
[6] Q. Li, S. Chen, W. Jiang, J. Appl. Polym. Sci. 103 (2007) 412–416.
[7] Z. Guo, S. Wei, B. Shedd, R. Scaffaro, T. Pereira, H.T. Hahn, J. Mater. Chem. 17 (2007) 806.
[8] S.A. Carter, J.C. Scott, P.J. Brock, Appl. Phys. Lett. 71 (1997) 1145.
[9] C.W. Lee, C. Renaud, C.S. Hsu, T.P. Nguyen, Nanotechnology 19 (2008) 455202.
[10] C. Ton-That, M.R. Phillips, T.-P. Nguyen, J. Lumin. 128 (2008) 2031–2034.

[11] N. Uekawa, N. Mochizuki, J. Kajiwara, F. Mori, Y.J. Wu, K. Kakegawa, Phys. Chem. Chem. Phys. 5 (2003) 929–934.
[12] L. Spanhel, M.A. Anderson, J. Am. Chem. Soc. 113 (1991) 2826–2833.
[13] V. Noack, A. Eychmüller, Chem. Mater. 14 (2002) 1411–1417.
[14] P. Hoyer, R. Eichberger, H. Weller, B. Bunsenges, Phys. Chem. 97 (1993) 630.
[15] T.R. Kuo, C.L. Wu, C.T. Hsu, W. Lo, S.J. Chiang, S.J. Lin, C.Y. Dong, C.C. Chen, Biomaterials 30 (2009) 3002–3008.
[16] K. Vanheusden, C.H. Seager, W.L. Warren, D.R. Tallant, J.A. Voigt, Appl. Phys. Lett. 68 (1996) 403.
[17] J.S. Kang, H.S. Kang, S.S. Pang, E.S. Shim, S.Y. Lee, Thin Solid Films 443 (2003) 5–8.
[18] N.V. Konoshchuk, L.N. Grebinskaya, V.D. Pokhodenko, Theor. Exp. Chem. 44 (2008) 339–344.
[19] H. Geng, Y. Guo, R. Peng, S. Han, M. Wang, Sol. Energy Mater. Sol. Cells 94 (2010) 1293–1299.
[20] R. Jetson, K. Yin, K. Donovan, Z. Zhu, Mater. Chem. Phys. 124 (2010) 417–421.
[21] G.D. Scholes, Annu. Rev. Phys. Chem. 54 (2003) 57.
[22] F. Massuyeau, E. Faulques, H. Athalin, S. Lefrant, J.L. Duvail, J. Wéry, E. Mulazzi, R. Perego, J. Chem. Phys. 130 (2009) 124706.
[23] N. Yamasaki, M. Watanabe, K. Masuyama, Y. Miyake, H. Kubo, A. Fujii, M. Ozaki, Jpn. J. Appl. Phys. 48 (2009) 101502.